


## ORIGINAL ARTICLE

# Circular RNA hsa\_circ\_0008003 promotes the progression of non-small-cell lung cancer by sponging miR-548I and regulating KPNA4 expression

Wenshu Yang | Yingying Yao | Shuai Yang  | Yaoqi Ke

Department of Respiratory and Critical Care Medicine, Xiang Yang Central Hospital, Affiliated Hospital of Hubei University of Arts and Science, Xiangyang, China

## Correspondence

Shuai Yang, Department of Respiratory and Critical Care Medicine, Xiang Yang Central Hospital, Affiliated Hospital of Hubei University of Arts and Science, No. 1 Zhongyuan Road, Fancheng District, Xiangyang, Hubei 441000, China.  
Email: yang1241979487@163.com

Yaoqi Ke, Department of Respiratory and Critical Care Medicine, Xiang Yang Central Hospital, Affiliated Hospital of Hubei University of Arts and Science, No. 1 Zhongyuan Road, Fancheng District, Xiangyang, Hubei 441000, China.  
Email: utosve@163.com

## Abstract

**Objective:** The study aimed to explore the effect of circ\_0008003 on the progression of non-small-cell lung cancer (NSCLC) and its underlying regulation mechanism.

**Methods:** Expression of hsa\_circ\_0008003, miRNA (miR)-548I and karyopherin subunit  $\alpha$  4 (*KPNA4*) was examined by quantitative real-time polymerase chain reaction. Cell viability and proliferation ability were detected by cell counting kit-8 assay and 5-ethynyl-2'-deoxyuridine assay, respectively. Flow cytometry was performed to monitor cell apoptosis. Western blot assay was used to evaluate the protein levels of *KPNA4*, Bax, and Bcl-2. Cell migration and invasion were assessed by transwell assays. The targeted relationship between miR-548I and hsa\_circ\_0008003 or *KPNA4* was confirmed by dual-luciferase reporter and RNA immunoprecipitation assays. Furthermore, the role of hsa\_circ\_0008003 in vivo was investigated by xenograft assay.

**Results:** Circ\_0008003 expression was increased in NSCLC tissues and cell lines. Circ\_0008003 knockdown reduced cell viability, migration, invasion, angiogenesis, and caused apoptosis in NSCLC cells. Moreover, miR-548I was targeted by circ\_0008003, and miR-548I knockdown reversed the influence of circ\_0008003 silence on NSCLC progression. *KPNA4* was targeted by miR-548I, and miR-548I overexpression suppressed cell viability, migration, invasion, angiogenesis, and promoted cell apoptosis via decreasing *KPNA4*. In addition, circ\_0008003 regulated *KPNA4* expression via miR-548I. Circ\_0008003 knockdown decreased NSCLC cell growth in the xenograft model.

**Conclusion:** Circular RNA hsa\_circ\_0008003 promoted progression in NSCLC by sponging miR-548I and regulating *KPNA4* expression, hinting that circ\_0008003 participates in NSCLC pathogenesis.

## KEYWORDS

circ\_0008003, *KPNA4*, miR-548I, NSCLC

## INTRODUCTION

Lung cancer is one of the most fatal malignant tumors in the world.<sup>1</sup> Most patients with lung cancer are non-small cell lung cancer (NSCLC).<sup>2</sup> Several researchers found that many risk factors can lead to NSCLC, including smoking, environmental pollution, food, and some lung-related

diseases.<sup>3</sup> Because of the lack of biomarkers for early diagnosis, treatment targets, and prognostic markers, cancer cells of most patients have metastasized before the consultation.<sup>4,5</sup> These challenges make it important to distinguish latent biomarkers for prognosis and to seek new targets for developing more reasonable treatments.

Circular RNAs (circRNAs) are a large class of noncoding RNAs with covalently closed-loop structures, which are rich, stable, and conservative.<sup>6</sup> Most of the circRNAs come from

Wenshu Yang and Yingying Yao contributed equally to this work.

This is an open access article under the terms of the [Creative Commons Attribution-NonCommercial-NoDerivs](https://creativecommons.org/licenses/by-nc-nd/4.0/) License, which permits use and distribution in any medium, provided the original work is properly cited, the use is non-commercial and no modifications or adaptations are made.

© 2022 The Authors. *Thoracic Cancer* published by China Lung Oncology Group and John Wiley & Sons Australia, Ltd.

the exon region of the gene, but a small part of them are formed by intron division.<sup>7</sup> CircRNA plays a significant role in plenty of human diseases, especially cancer-related diseases.<sup>8</sup> Previous studies have suggested that circRNAs can act as “microRNAs (miRNA) sponges” and participate in the regulation of tumor progress.<sup>9–12</sup> Hu et al. found that circ\_0008003 can participate in the regulation of the occurrence and development of NSCLC, and part of this is to act as a sponge of mir-488, which was proven to be a tumor suppressor in some tumor diseases.<sup>13,14</sup> Although some studies have proposed relevant molecular mechanisms of circRNAs and miRNAs in NSCLC, further studies are needed to elucidate the regulatory network of circRNAs and their downstream factors.

This study is the first to detect the correlation between circ\_0008003 and miR-548I. This study revealed the role of circ\_0008003 in the proliferation, migration, apoptosis, and tumor growth of NSCLC and explored its downstream signal axis.

## MATERIALS AND METHODS

### Sample collection

A total of 30 pairs of human NSCLC tissues and paracancerous tissues were collected from patients with NSCLC at Xiang Yang Central Hospital, Affiliated Hospital of Hubei University of Arts and Science between 2016 and 2021. The age of all patients ranged from  $50 \pm 5$  years. The subjects were informed and the study was approved by the ethics committee of Xiang Yang Central Hospital, Affiliated Hospital of Hubei University of Arts and Science. The specimens were selected and the patient consent was obtained in advance.

### Cell culture and cell transfection

Human bronchial epithelial cell line (16HBE) and two NSCLC cell lines (H1299 and A549) were obtained from Chuan Qiu Biotechnology. All the cells were cultured in Dulbecco's modified Eagle medium medium at 37°C with 5% CO<sub>2</sub>. The small interfering RNA circ\_0008003 (si-circ\_0008003), miR-548I mimic, miR-548I inhibitor, and negative controls (miRNA NC, inhibitor NC) were synthesized by GenePharma. The plasmid overexpressing karyopherin subunit  $\alpha$  4 (KPNA4) (pc-KPNA4) and negative control (pc-NC) were purchased from RiboBio. According to the manufacturer's instructions, Lipofectamine 3000 (Invitrogen) was used for transfection experiments.

### RNA extraction and quantitative real-time polymerase chain reaction

Total RNA was isolated and extracted by Trizol reagent (Invitrogen). After RNA was reverse transcribed, quantitative real-time polymerase chain reaction (qRT-PCR) was

**TABLE 1** Primers sequences used for PCR

Name	Sequences (5'-3')
Circ_0008003	F: CCTCAACTACCTCAGGGAGGC R: GAAAGGGTTAATGTGGCGTCA
miR-548I	F: GCCGAGAAAAGTAATTGCGGAT R: GTGCAGGGTCCGAGGT
KPNA4	F: GCACTCCTGACACATCCCAA R: TGCCAAAATCCCCCTTATCCA
LDB2	F: ACTATCGGCAGGACCCTCAT R: ATGGTACACTGGTCGACGC
GAPDH	F: TCGGAGTCAACGGATTGGT R: TTCCTGTTCTCAGCCTTGAC
U6	F: CTCGCTTCGGCAGCACATA R: CGAATTTGCGTGTTCATCCT

Abbreviations: glyceraldehyde 3-phosphate dehydrogenase; KPNA4, karyopherin subunit  $\alpha$  4; LDB2, LIM domain-binding 2; miR, microRNA.

performed. The primers used in the current tests were designed by premier 5.0 software and purchased from Sangon Biotech (Table 1). qRT-PCR experiments using the SYBR Green mix (Kakara) were executed on ABI 7500 fast PCR System (Applied Biosystems). U6 and glyceraldehyde 3-phosphate dehydrogenase (GAPDH) were used as internal standard control. The relative expression levels of molecules were assessed with the  $2^{-\Delta\Delta CT}$  method.

### Hematoxylin and eosin staining

NSCLC tissues and normal lung tissues were fixed in 4% paraformaldehyde and dehydrated with different concentrations of alcohol. After that, 5- $\mu$ m sections were stained with hematoxylin and eosin (H&E) solution (Invitrogen). A microscope was used to analyze the staining results.

### Cell counting kit-8 assay

Cell counting kit-8 (CCK-8) assay was used to evaluate cell viability. The cells were seeded in 96-well plates (5000 cells per well). Before testing, 10  $\mu$ L CCK-8 reagent (Dojindo) was added into each well. When the incubation was completed, the absorbance of each well was measured and recorded at 490 nm by using a Varioskan Flash system (Thermo Fisher Scientific).

### 5-Ethynyl-2'-deoxyuridine assay

According to the 5-ethynyl-2'-deoxyuridine (EdU) proliferation kit (RiboBio) instructions, 48 h after transfection, the cells were treated with 50 mmol/L EdU for 2 h. Next, the cells were sealed with 4', 6-diamidino-2-phenylindole (DAPI). EdU-positive cells were observed by fluorescence microscope. Image J (National Institutes of Health) was used to calculate the cell proliferation rate.

## Transwell analysis

Cell migration and invasion ability were detected by transwell assay. First,  $5 \times 10^5$  cells were suspended with serum-free medium and added into the upper chamber pre-coated with the Matrigel (Solarbio) for invasion assay, or without Matrigel for migration assay. The culture medium with 10% serum was added into the inferior chamber. After incubation for 24 h, the cells were stained with crystal violet (Solarbio), washed, and counted under microscope (Olympus).

## Angiogenesis test

Matrigel was used for the angiogenesis test. A549 cells or H1299 cells were seeded into a 24-well plate ( $2 \times 10^3$  cells/well) coated with Matrigel. After incubation for 6–8 h, the cells were observed using a microscope (Olympus), and Image J software was used to measure the number of tubes.

## Cell apoptosis assay

Cell apoptosis was detected by an apoptosis analysis kit (Servicebio). Briefly, cells were suspended in the flow cytometry binding buffer and stored with Annexin V/fluorescein isothiocyanate and propidium iodide in the absence of light for 20 min at 25°C. The apoptotic rates were analyzed using FlowJo 7.6 software.

## Western blot assay

Total proteins were extracted from tissues or cells with radio-immunoprecipitation assay buffer cell lysate (Beyotime) and quantified. The extracted protein was separated by sodium dodecyl sulfate-polyacrylamide gel electrophoresis gel and transferred to polyvinylidene fluoride membranes. After being blocking with 5% skimmed milk powder, the membrane was incubated with the KPNA4 antibody (ab176585, Abcam), Bcl-2 antibody (ab182858, Abcam), Bax antibody (ab32503, Abcam), GAPDH antibody (ab8245, Abcam), at 4°C overnight. The membrane was then incubated with the second antibody for 1 h. Enhanced chemiluminescence (ECL) solution (Thermo Fisher Scientific) was used to expose the band, and Image J software was used to analyze.

## Dual-luciferase reporter analyses

The targets of circ\_0008003 and miR-548I were predicted by Circinteractome website and Starbase website, respectively. Dual-luciferase reporter analyses were conducted to study the target correlation of miR-548I and circ\_0008003 or KPNA4. The wild-type (WT-circ\_0008003 or WT-KPNA4-3'UTR) or mutant luciferase reporter vectors (MUT-circ\_0008003 or MUT-KPNA4-3'UTR) were cloned by inserting the corresponding sequence containing WT or MUT miR-548I complementary sites into psiCHECK2 vector (Hanbio Biotechnology) via endonuclease. The vectors and miR-548I mimic or miRNA NC were transfected into

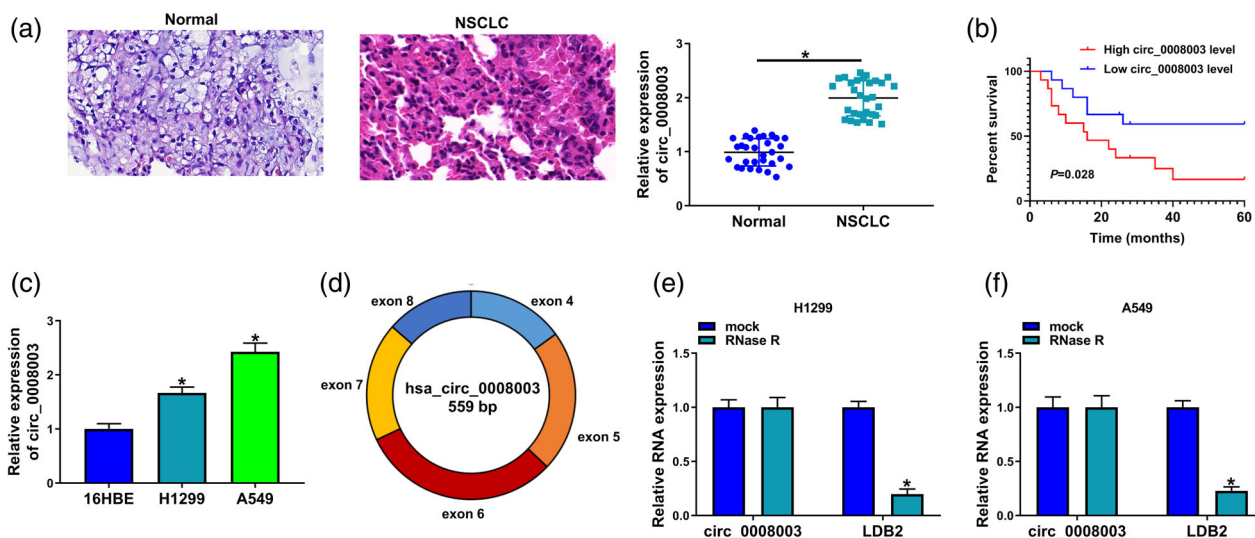


**FIGURE 1** The expression of circ\_0008003 was increased in NSCLC tissues and cell lines. (a) The pathological conditions of NSCLC tissues were analyzed by H&E staining, and circ\_0008003 expression was detected by qRT-PCR in 30 paired samples of NSCLC tissues. (b) Kaplan–Meier methods were used to analyze the overall survival curve of NSCLC patients with high or low circ\_0008003 expression. NSCLC patients were divided into the high circ\_0008003 expression group and low circ\_0008003 expression group by median circ\_0008003 expression. (c) Circ\_0008003 expression was detected by qRT-PCR in cell lines (16HBE, A549, H1299). (d) Circ\_0008003 is produced at the LDB2 gene locus containing exons 4–8. (e) and (f) qRT-PCR analysis for the expression of circ\_0008003 and LDB2 after treatment with RNase R in NSCLC cells (A549 and H1299). NSCLC, non-small cell lung cancer; H&E, hematoxylin and eosin; qRT-PCR, quantitative real-time polymerase chain reaction

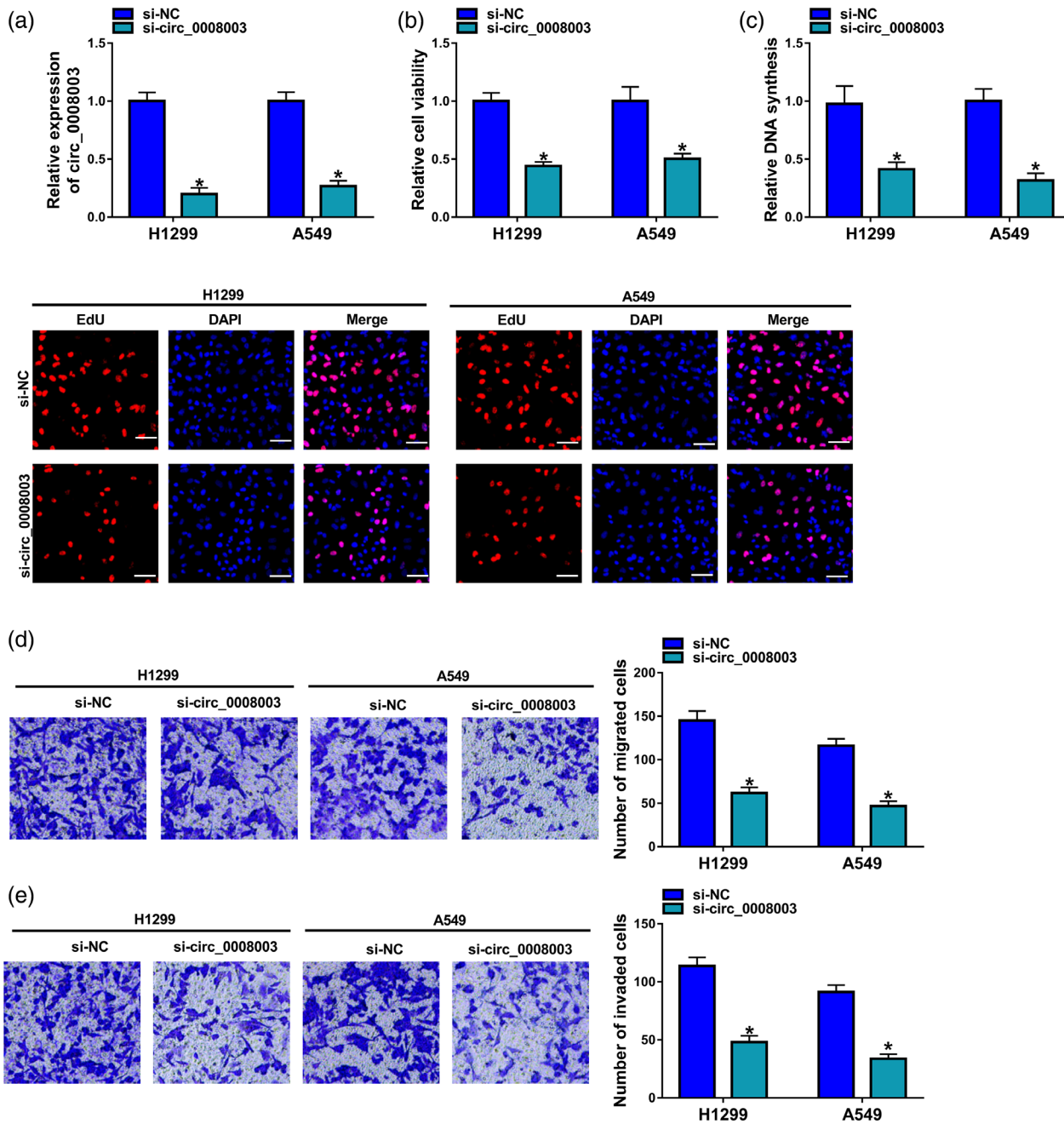


**FIGURE 2** Circ\_0008003 knockdown hindered the proliferation, migration, and invasion of NSCLC cells. (a) Circ\_0008003 level was detected by qRT-PCR in si-NC or si-circ\_0008003 transfected cells. (b) CCK-8 assay was performed to evaluate cell viability in NSCLC cells. (c) EdU assay was performed to detect the proliferative ability of NSCLC cells. (d), (e) The capabilities of transfected cells to migrate and invade were assessed via transwell. NSCLC, non-small cell lung cancer; qRT-PCR, quantitative real-time polymerase chain reaction; si, small interfering; NC, negative control; CCK-8, cell counting kit-8; EdU, 5-ethynyl-2'-deoxyuridine

A549 or H1299 cells for 24 h. The luciferase activity was detected by dual luciferase reporter assay system (Promega).

### RNA immunoprecipitation assay

RNA immunoprecipitation (RIP) analysis was performed with a Magna RIP kit (Millipore). RIP buffer was used to lyse NSCLC cells, and then the lysate was incubated with magnetic beads bound with anti-ago2 antibody (Bioss) or

anti-IgG antibody. Subsequently, the immunoprecipitated RNA was extracted, and the relative expression of RNA was analyzed by qRT-PCR experiment.

### Tumor xenograft in nude mice

Before the experiment, the animal experiment was authorized by the animal research ethics committee of Xiang Yang Central Hospital, Affiliated Hospital of Hubei University of

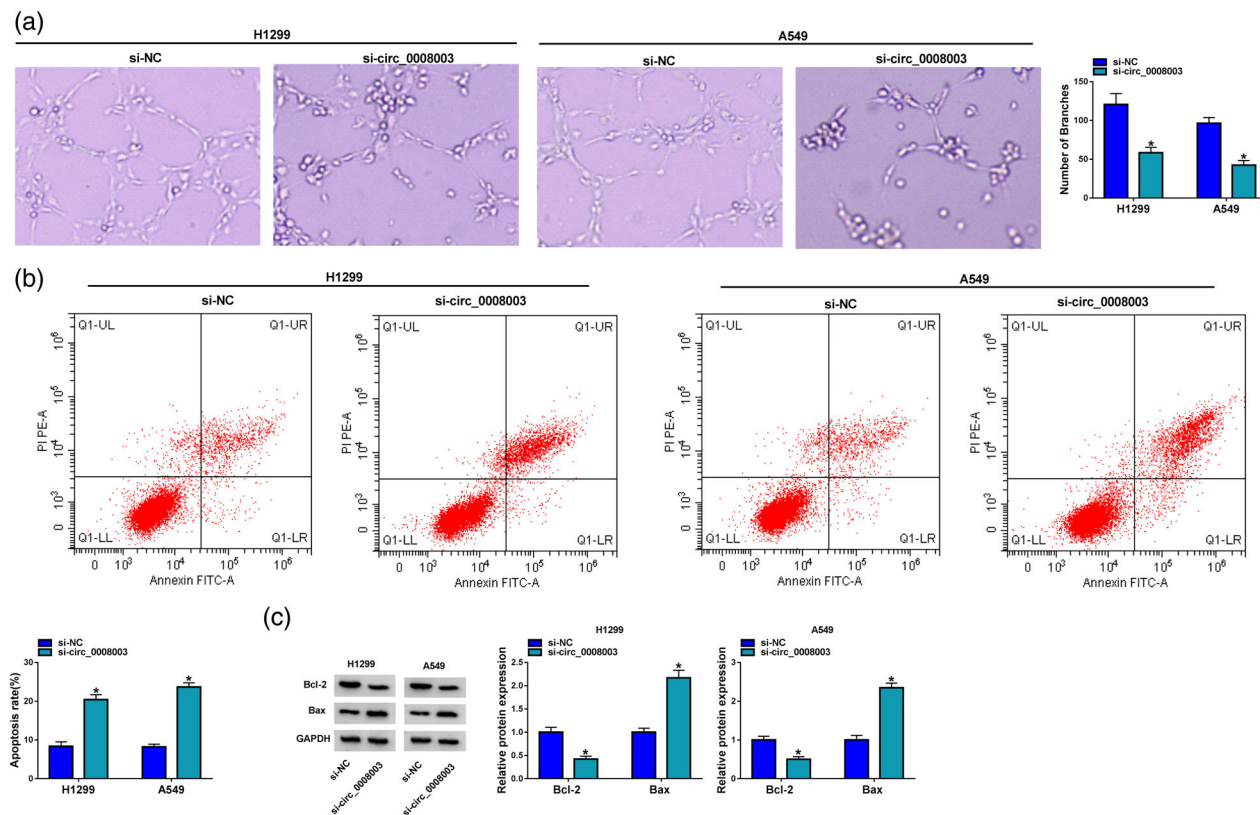


**FIGURE 3** Circ\_0008003 knockdown promoted the apoptosis of NSCLC cells. (a) Tube formation assay was used to detect the tube formation ability of human umbilical vein endothelial cells in transfected NSCLC cells. (b) Flow cytometry assay was conducted to test NSCLC cell apoptosis rate. (c) Western blot assay was implemented to determine the protein levels of Bax and Bcl-2. NSCLC, non-small cell lung cancer

Arts and Science. Twelve nude mice (6 mice per group, male, 6 weeks old) were randomly divided into two groups (short hairpin [sh]-NC group and sh-circ\_0008003 group). Mice were subcutaneously injected with  $1 \times 10^6$  A549 cells transfected with sh-circ\_0008003 or sh-NC. The tumor size was measured every week. All mice were euthanized on the 35th day after injection. The tumor volume and weight were measured and the related expression levels were analyzed by qRT-PCR and western blot. In addition, the expression of cell proliferation marker Ki67 in tumor tissues was analyzed by immunohistochemistry (IHC).

## Immunohistochemistry

IHC experiments were carried out according to the classical procedure. In brief, after the slices were washed three times with phosphate buffered saline, the sections were incubated with primary antibody Ki67 (1:100, ab15580, Abcam). The corresponding secondary antibody HRP (1:500, ab205718) was added and incubated for 30 min. The slices were immersed in methanol solutions containing 10% hydrogen peroxide for 10 min. Next, after glyceraldehyde 3-phosphate dehydrogenase (DAB) development and hematoxylin re staining, the slices were washed with distilled water. After

dehydration and transparency, the slices were sealed with neutral resin. Immunohistochemical images were analyzed by microscope.

## Statistical analysis

*t*-Test was used to compare the difference between the groups. ANOVA analysis method was used for the comparison of more than two groups. GraphPad Prism 7.0 software was used for graph drawing, and  $p < 0.05$  was considered to be significant. Every test was repeated three times independently.

## RESULTS

### Circ\_0008003 was up-regulated in NSCLC tissues and cells

Thirty pairs of NSCLC tissues and controlled peritumor tissues were used to analyze the expression of circ\_0008003 by qRT-PCR. The expression level of circ\_0008003 was significantly upregulated in tumor tissues compared with control (Figure 1(a)). NSCLC patients with high circ\_0008003 expression had low survival rates in comparison with the

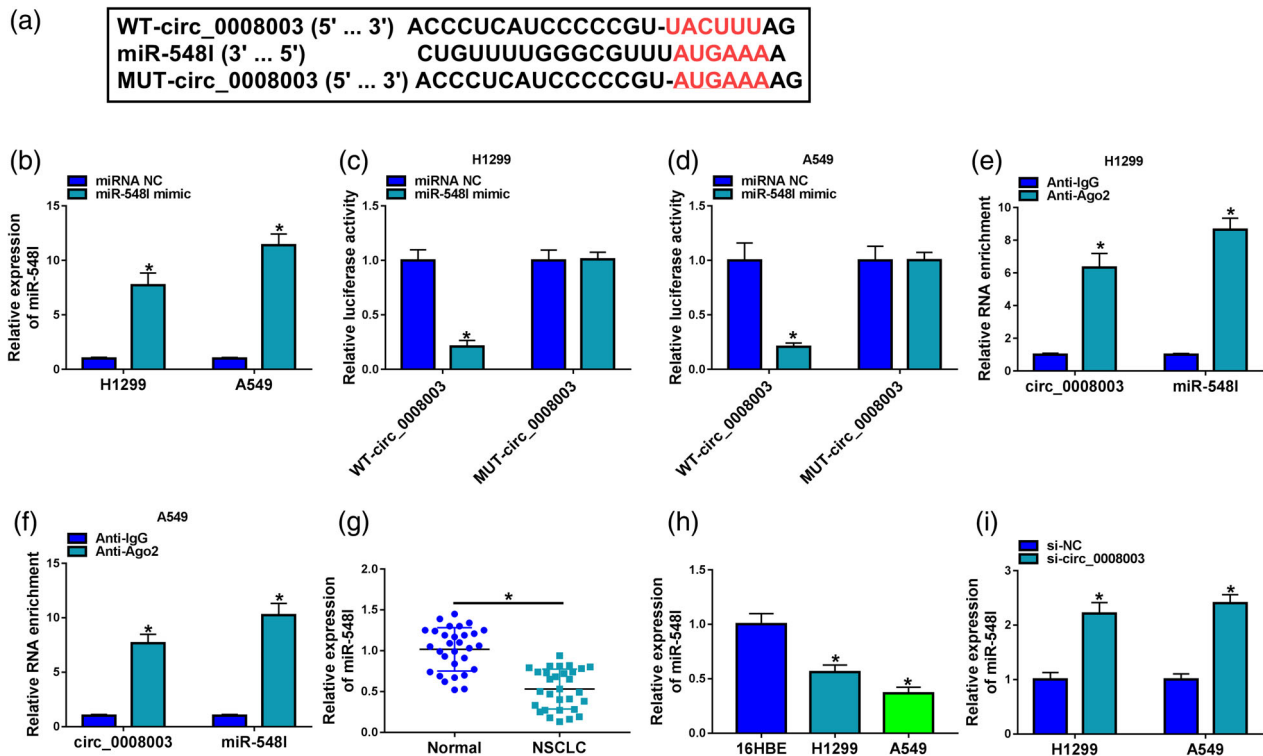


**FIGURE 4** MiR-548I was the potential target of circ\_0008003 in NSCLC cells. (a) The bioinformatic analysis of the binding site of miRNA-548I and circ\_0008003. (b) The relative levels of miR-548I expression in NSCLC cells were determined with qRT-PCR. (c), (d) Luciferase activity was measured after co-transfecting with circ\_0008003 plasmid and miR-548I mimic. (e) and (f) RIP assay was performed to verify the interaction of circ\_0008003 and miR-548I. (g), (h) The expression of miR-548I in NSCLC tissues and cells was detected by qRT-PCR. (i) qRT-PCR was performed to detect the expression of miR-548I in circ\_0008003 downregulation cells. NSCLC, non-small cell lung cancer; miRNA, microRNA; qRT-PCR, quantitative real-time polymerase chain reaction; RIP, RNA immunoprecipitation

patients with low circ\_0008003 expression (Figure 1(b)). Circ\_0008003 was significantly upregulated in NSCLC cells (A549, H1299) compared to 16HBE cells (Figure 1(c)). Circ\_0008003 is derived from regions of exons 4–8 of LDB2 messenger RNA (mRNA), with short introns between each exon (Figure 1(d)). In addition, resistance to digestion by RNase R exonuclease further confirmed the circular form and loop structure of hsa\_circ\_0008003 (Figure 1(e),(f)). Taken together, hsa\_circ\_0008003 was identified as a potential regulator in NSCLC.

### Knockdown of circ\_0008003 restrained cellular proliferation, migration, and invasion, angiogenesis and promoted cell apoptosis

The expression of circ\_0008003 in A549 and H1299 cells was reduced significantly after A549 and H1299 cells were transfected with si-circ\_0008003 (Figure 2(a)). Knockdown circ\_0008003 significantly inhibited proliferation activity (Figure 2(b),(c)). The transwell assay data indicated that cell migration and invasion were impaired by circ\_0008003 silencing (Figure 2(d),(e)). Tube formation assay also demonstrated that the angiogenesis of A549 and H1299 cells was weakened after circ\_0008003 expression was silenced

(Figure 3(a)). In addition, as shown in Figure 3(b), the apoptosis rate of the si-circ\_0008003 group was markedly higher than that of the si-NC group. In support, we found low expression of Bcl-2 and high expression of Bax after circ\_0008003 silencing in A549 and H1299 cells (Figure 3(c)). Collectively, these results suggested that circ\_0008003 promoted NSCLC progress.

### Circ\_0008003 served as a sponge for miR-548I

To further study the potential downstream miRNA of circ\_0008003, circRNA interactome online prediction website showed miR-548I was a potential targeting miRNA of circ\_0008003 (Figure 4(a)). We found that miR-548I mimics significantly increased miR-548I expression (Figure 4(b)). A significant reduction in luciferase reporter activity of the WT-circ\_0008003 + miR-548I mimic group was observed relative to co-transfection with miRNA NC (Figure 4(c), (d)). Next, we performed RIP with an anti-AGO2 antibody in the A549 and H1299 cell lines. Our results showed that circ\_0008003 and miR-548I were significantly enriched, because they were precipitated by the anti-AGO2 antibody (Figure 4(e),(f)). Collectively, these results suggested that circ\_0008003 acted as a binding platform for miR-548I.

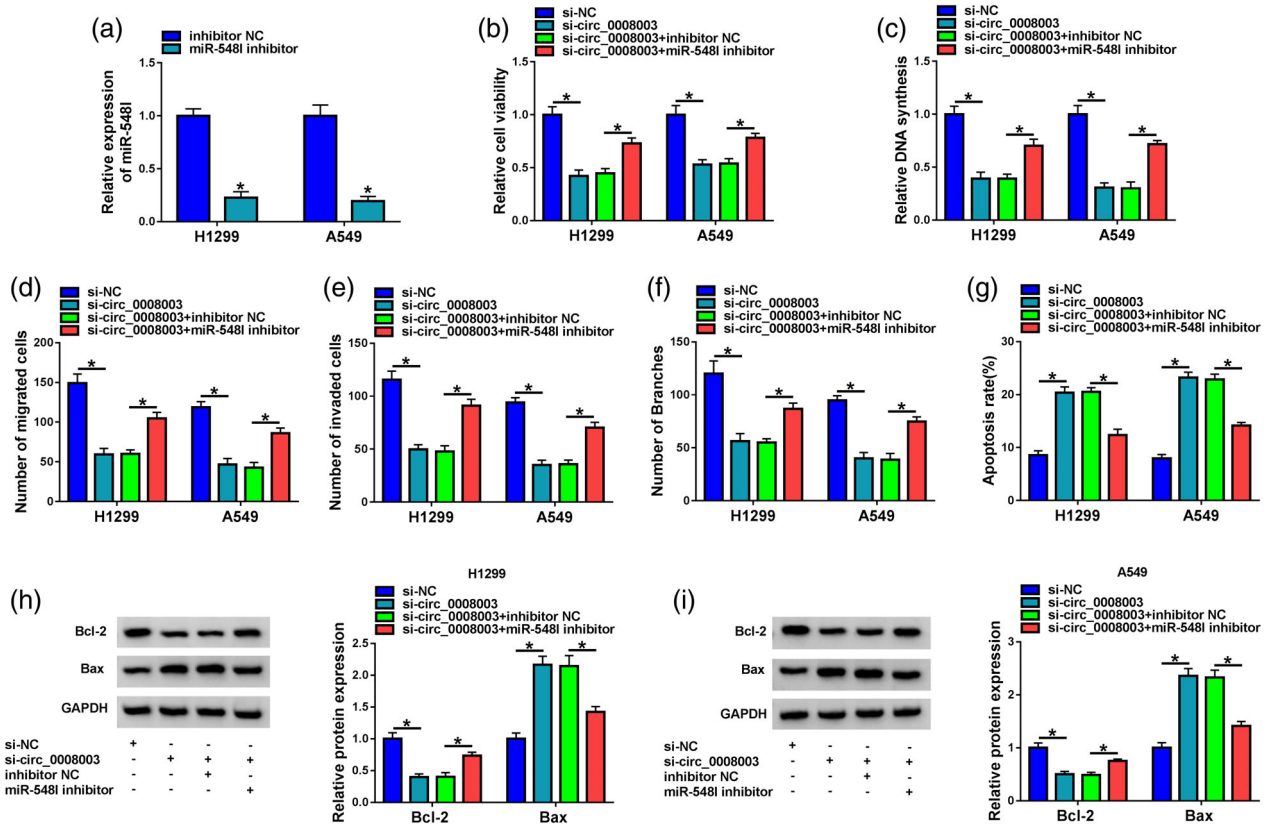


**FIGURE 5** miR-548I reversed the effects of circ\_0008003 on NSCLC cells. (a) The expression level of miR-548I was analyzed by qRT-PCR. (b), (c) CCK-8 assay and EdU assay were performed to determine the proliferation. (d), (e) Transwell assay was used to analyze the migration and invasion ability of NSCLC cells. (f) Tube formation assay for the angiogenesis of transfected cells. (g) Flow cytometry for the apoptotic rate of transfected cells. (h), (i) Western blot assay for the protein levels of Bax and Bcl-2 in transfected cells. MiR, microRNA; NSCLC, non-small cell lung cancer; qRT-PCR, quantitative real-time polymerase chain reaction; CCK-8, cell counting kit-8; EdU, 5-Ethynyl-2'-deoxyuridine

qRT-PCR showed the expression level of miR-548I was significantly reduced in tumor tissue compared with control (Figure 4(g)). miR-548I was significantly downregulated in NSCLC cells (A549 and H1299) compared to 16HBE cells (Figure 4(h)). Furthermore, data exhibited that miR-548I expression was increased after circ\_0008003 knockdown (Figure 4(i)).

### miR-548I inhibition restored the effects of circ\_0008003 on cell proliferation, migration, invasion, angiogenesis, and apoptosis in NSCLC cells

Based on the foregoing finding that circ\_0008003 may exert its function through direct interaction with miR-548I, miR-548I expression was measured after regulating miR-548I level. The miR-548I expression was decreased by miR-548I inhibitor (Figure 5(a)). Further analyses revealed that si-circ\_0008003 led to a striking repression in cell proliferation (Figure 5(b),(c)), migration, invasion (Figure 5(d),(e)), angiogenesis (Figure 5(f)), and a distinct enhancement in cell apoptosis (Figure 5(g)), as well as increased Bax protein expression level and decreased

Bcl-2 protein expression level (Figure 5(h),(i)). Moreover, these effects were remarkably reversed by inhibiting miR-548I expression.

### miR-548I interacted with *KPNA4* in NSCLC cells

Through analyzing of StarBase database, we found that there was a binding site between *KPNA4* 3'UTR and miR-548I (Figure 6(a)). Dual-luciferase reporter assay showed that the luciferase activity of WT-*KPNA4*-3'UTR + miR-548I group was dramatically decreased in A549 and H1299 cells, but the luciferase activity of MUT-*KPNA4*-3'UTR and miR-548I co-transfected group was not changed (Figure 6(b),(c)). RIP assay revealed that miR-548I and *KPNA4* were dramatically enriched in anti-Ago2 group compared with the anti-IgG group (Figure 6(d),(e)). Moreover, *KPNA4* was highly expressed in NSCLC tissues (Figure 6(f),(g)) and cells (Figure 6(h)) than in healthy tissues and 16HBE cells. Additionally, overexpression of miR-548I decreased the protein levels of *KPNA4* in NSCLC cell lines (Figure 6(i)). These results suggested that *KPNA4* is the downstream target gene of miR-548I.

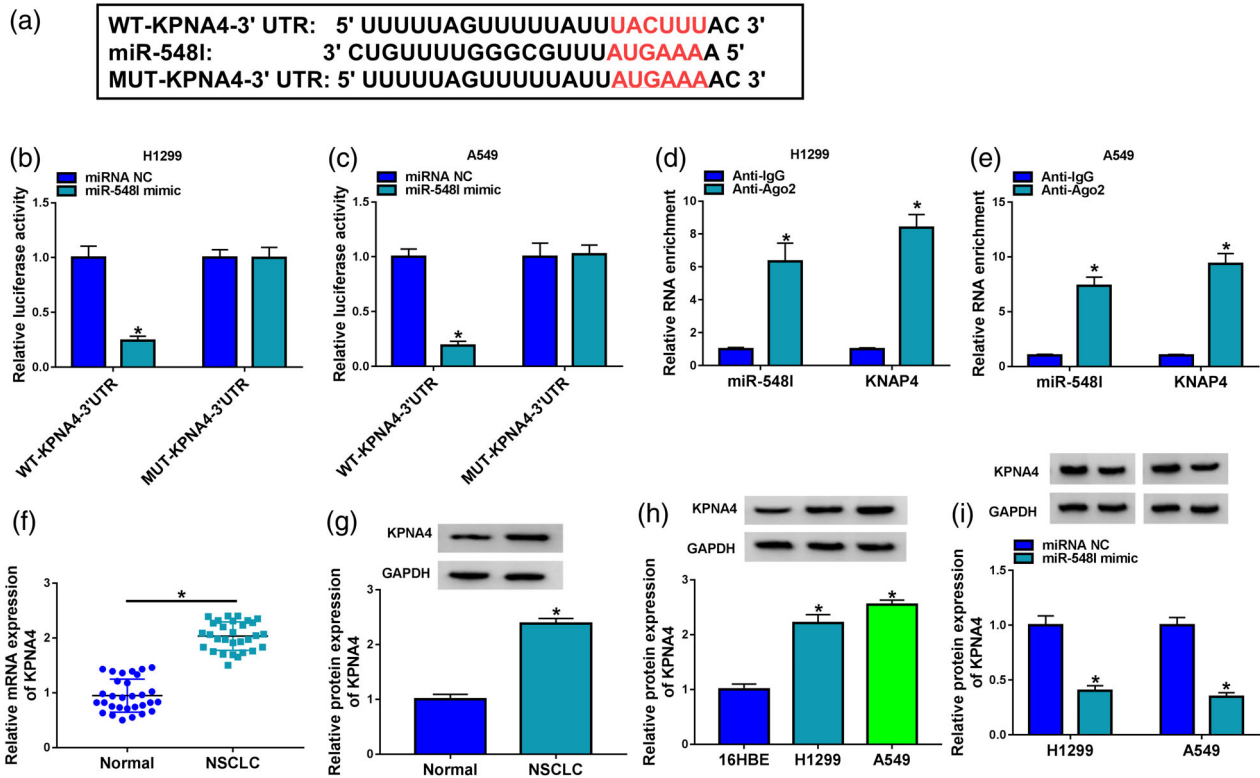


**FIGURE 6** *KPNA4* was a direct target of miR-548I. (a) Putative miR-548I binding site in the 3'-UTR of *KPNA4* is shown. (b), (c) Dual-luciferase reporter assay was performed to confirm the binding site of *KPNA4* and miR-548I. (d), (e) RIP assay was used to test the combination of *KPNA4* and miR-548I. (f) The mRNA expression of *KPNA4* and corresponding normal tissues were detected by qRT-PCR. (g), (h) The protein level of *KPNA4* in NSCLC patients and cell were measured by western blot. (i) Western Blot was used to detect the expressions of *KPNA4* in NSCLC cells. *KPNA4*, karyopherin subunit  $\alpha$  4; MiR, microRNA; RIP, RNA immunoprecipitation; mRNA, messenger RNA; qRT-PCR, quantitative real-time polymerase chain reaction; NSCLC, non-small cell lung cancer

## MiR-548 axis regulated the progression of NSCLC by targeting *KPNA4*

As mentioned above, we next investigated the functional mechanism between miR-548I and *KPNA4*. The protein expression levels of *KPNA4* were increased in NSCLC cells transfected with pc-*KPNA4* (Figure 7(a)). As shown in Figure 7(b)–(g), miR-548I overexpression obviously inhibited cell viability, migration, invasion, and angiogenesis of NSCLC cells, but accelerates cell apoptosis rates. However, the addition of *KPNA4* overexpression vector was able to reverse the effect of miR-548I mimic on the NSCLC cells. The data of western blot assay exhibited that miR-548I mimic markedly reduced the levels of Bcl-2 and increased the levels of Bax in NSCLC cells, whereas upregulation of *KPNA4* partly reversed the change (Figure 7(h),(i)). All results confirmed that miR-548I regulated NSCLC progression by targeting *KPNA4*.

## *KPNA4* expression was regulated by circ\_0008003 and miR-548I

Based on the above research, we explored whether circ\_0008003 could regulate *KPNA4* expression by acting as

a sponge of miR-548I in NSCLC cells. The data showed that circ\_0008003 downregulation reduced *KPNA4* protein expression, whereas miR-548I inhibition reversed the inhibitory effect of circ\_0008003 knockdown on *KPNA4* protein expression (Figure 8).

## Knockdown of circ\_0008003 inhibited NSCLC progression

Finally, we tested the impact of circ\_0008003 knockdown on tumor growth in vivo. Tumor growth and volume were measured. Results showed that tumor growth and volume were slower and smaller in sh-circ\_0008003 group than that in sh-NC group (Figure 9(a),(b)). qRT-PCR showed that silencing of circ\_0008003 downregulated circ\_0008003 level and upregulated miR-548I level. Western blot detection of *KPNA4* expression in tumors showed that silencing of circ\_0008003 downregulated *KPNA4* (Figure 9(c)–(e)). IHC assay showed that the knockdown of circ\_0008003 decreased *KPNA4* and Bax expression but increased Bcl-2 expression in tumors (Figure 9(f)). Taken together, these findings demonstrated that circ\_0008003 was an oncogene that exerted its functions by regulating the miR-548I/*KPNA4* axis in NSCLC in vivo.



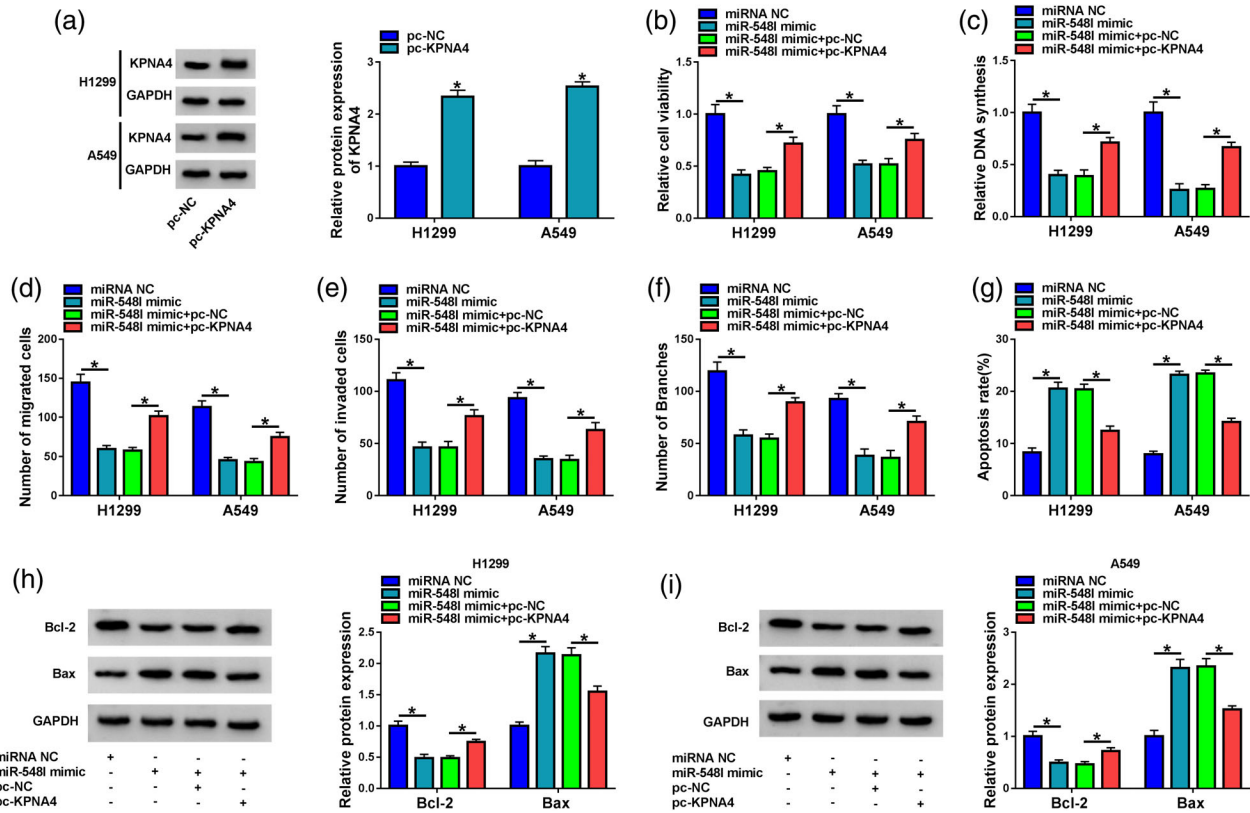


**FIGURE 7** miR-548I repressed proliferation and migration and induced apoptosis of NSCLC cells by regulating KPNA4. (a) The protein expression of KPNA4 was detected by western blot in NSCLC cells. (b), (c) Cell proliferation viability was measured by CCK-8 assay and EdU assay. (d), (e) The influence of miR-548I and KPNA4 on cell migration and invasion of NSCLC cells measured by transwell assay. (f) Tube formation assay for the angiogenesis of transfected cells. (g) Cell apoptosis was determined by flow cytometry assay. (h), (i) The expression of Bax and Bcl-2 was determined by western blot. MiR, microRNA; NSCLC, non-small cell lung cancer; KPNA4, karyopherin subunit  $\alpha$  4; CCK-8, cell counting kit-8; EdU, 5-ethynyl-2'-deoxyuridine

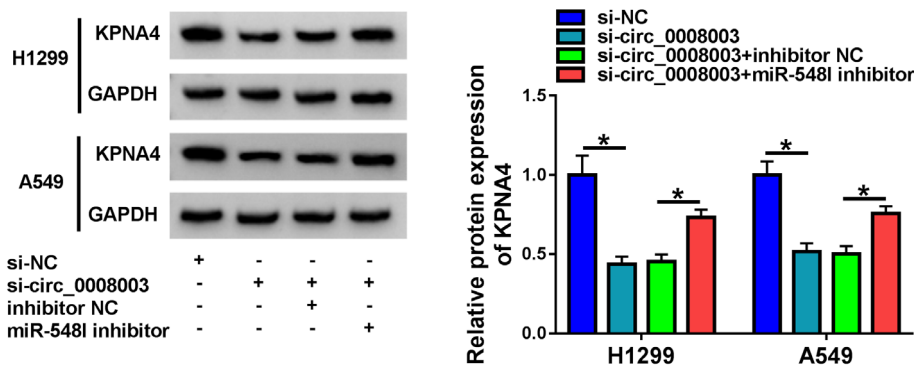


**FIGURE 8** Circ\_0008003 positively regulated KPNA4 by sponging miR-548I in NSCLC cells. Western blotting was used to detect KPNA4 protein expression in NSCLC cells. KPNA4, karyopherin subunit  $\alpha$  4; NSCLC, non-small cell lung cancer

**DISCUSSION**

With the rapid development of science and biotechnology, many researchers are focusing attention on circRNAs. The study of circRNAs has led to some surprising findings, indicating that circRNAs regulate a wide range of pathological processes, especially in tumorigenesis.<sup>15-17</sup> Hence, circRNA-based diagnostic and therapeutic strategies may bring into play prospective functions in cancer treatment.

A previous report revealed that circ\_0008003 participated in NSCLC progress, and circ\_0008003 promotes

NSCLC cell invasion and proliferation in vitro.<sup>13</sup> Consistently, this study also found that the expression of circ\_0008003 was highly expressed in NSCLC tissues and cells. NSCLC patients with high circ\_0008003 expression had low survival rates. Moreover, our data indicated that circ\_0008003 can induce proliferation and suppress apoptosis of NSCLC cells in vitro. Furthermore, circ\_0008003 also accelerated tumor growth in vivo.

The mechanism of competing endogenous RNA (ceRNA) is one of the important ways for circRNAs to function. For instance, Wang et al.<sup>18</sup> found that circP4HB

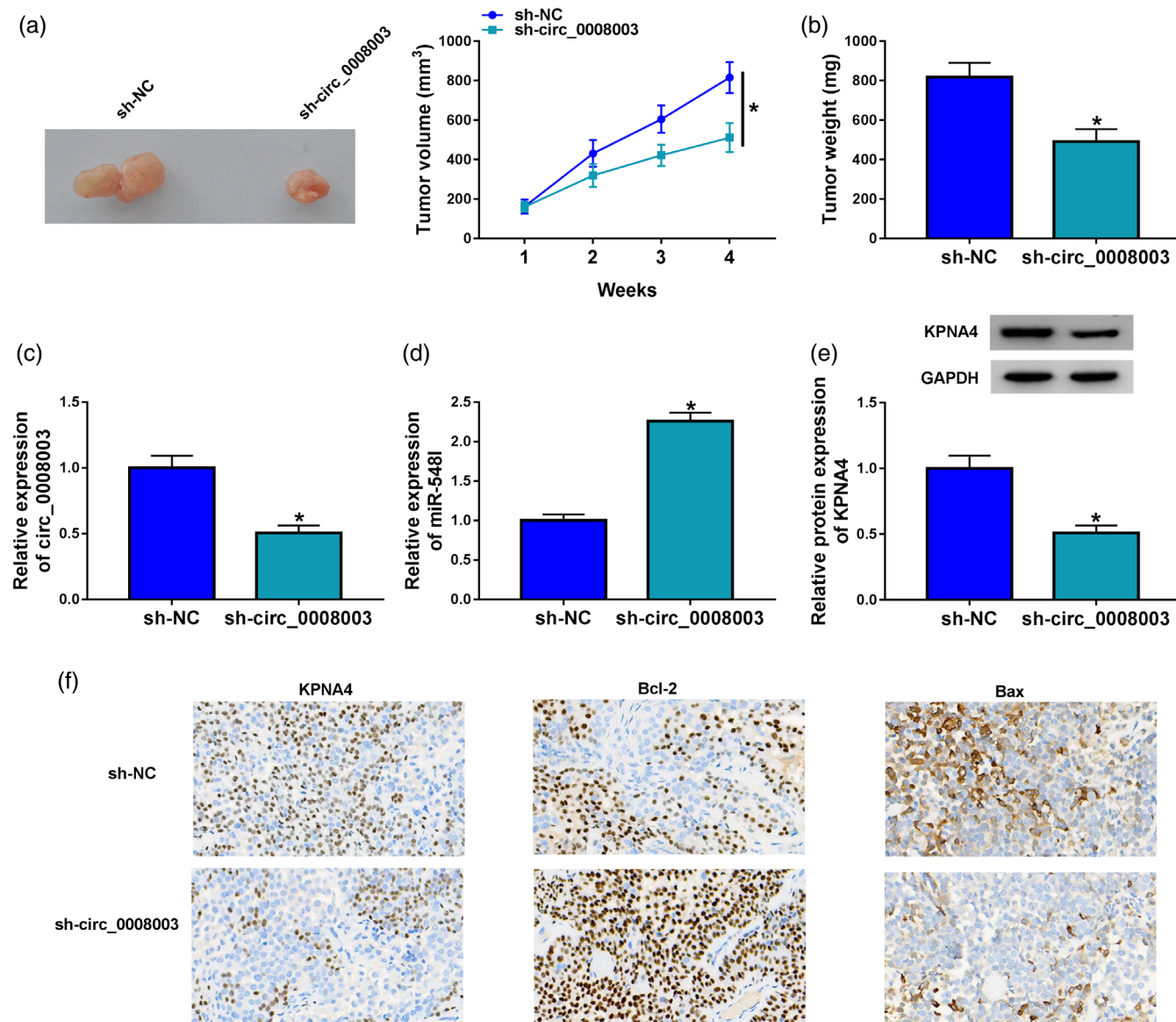


**FIGURE 9** Circ\_0008003 significantly affected tumor growth in vivo. (a), (b) The tumor volume (a) and weight (b) in mice were determined. (c), (d) The relative levels of circ\_0008003 and miR-548l in tumor tissues were determined by qRT-PCR. (e) The relative levels of KPNA4 protein expression in tumor tissues were determined by western blot. (f) Immunohistochemistry staining was used to determine the expression of KPNA4, Bcl-2 and Bax in tissues from mice. qRT-PCR, quantitative real-time polymerase chain reaction; KPNA4, karyopherin subunit  $\alpha$  4

promoted cell metastasis in vitro through the sequestration of miR-133a-5p. Circ\_103809 increased cisplatin-resistance of the A549 and H1299 cells by regulating miR-377-3p in NSCLC.<sup>19</sup> In the current study, we speculated whether circ\_0008003 functioned by acting as a miR-548l sponge. The experimental data revealed that circ\_0008003 played a carcinogenic role via sponging miR-548l in NSCLC.

These miRNAs are essential regulators of gene expression and usually inhibit mRNA translation.<sup>20,21</sup> In this research, we found that downregulating miR-548l partially reversed the inhibitory effects of circ\_0008003 knockdown on NSCLC progression. Liu et al.<sup>22</sup> found that overexpression of miR-548l suppressed NSCLC cell migration and invasion. Moreover, circNFATC3 can sponge miR-548l to

regulate hepatocellular carcinoma progression.<sup>23</sup> *KPNA4* has been proven to be a kind of mRNA with the potential to promote tumorigenesis and the development of a variety of human malignant tumors.<sup>24,25</sup> *KPNA4* expression counteracts the inhibitory effect of silenced circCCDC66 on the progression of NSCLC.<sup>26</sup> Overexpression of *KPNA4* partially counteracts the inhibitory effect of MCM3AP-AS1 gene knockout on angiogenesis and progression of lung cancer cells.<sup>27</sup> In the present study, circ\_0008003 primarily mediated its promotion effect on NSCLC progression by sponging miR-548l to regulate *KPNA4* expression.

Taken together, we conclude that circ\_0008003 overexpression increases the release of *KPNA4* by sponging miR-548l, further promoting NSCLC cell progression.

Circ\_0008003/miR-548I/KPNA4 regulatory network may become a potential therapeutic target for NSCLC patients.

## AUTHOR CONTRIBUTIONS

Wenshu Yang designed and performed the research. Shuai Yang and Yaoqi Ke analyzed the data. Wenshu Yang and Yingying Yao wrote the manuscript. All authors read and approved the final manuscript.

## DISCLOSURE OF INTEREST

The authors declare that they have no conflict of interest.

## ETHICS APPROVAL AND CONSENT TO PARTICIPATE

Written informed consents were obtained from all participants and this study was permitted by the Ethics Committee of Xiang Yang Central Hospital, Affiliated Hospital of Hubei University of Arts and Science.

## ORCID

Shuai Yang  <https://orcid.org/0000-0002-4323-5921>

## REFERENCES

- Sung H, Ferlay J, Siegel RL, Laversanne M, Soerjomataram I, Jemal A, et al. Global cancer statistics 2020: Globocan estimates of incidence and mortality worldwide for 36 cancers in 185 countries. *CA-Cancer J Clin.* 2021;71:209–49.
- Hong QY, Wu GM, Qian GS, Hu CP, Zhou JY, Chen LA, et al. Prevention and management of lung cancer in China. *Cancer.* 2015;121(Suppl 17):3080–8.
- Sudhindra A, Ochoa R, Santos ES. Biomarkers, prediction, and prognosis in non-small-cell lung cancer: a platform for personalized treatment. *Clin Lung Cancer.* 2011;12:360–8.
- Rotoli D, Santana-Viera L, Ibba ML, Esposito CL, Catuogno S. Advances in oligonucleotide aptamers for NSCLC targeting. *Int J Mol Sci.* 2020;21:6075.
- Tian Y, Xu J, Chu Q, Duan J, Zhang J, Bai H, et al. A novel tumor mutational burden estimation model as a predictive and prognostic biomarker in nscl patients. *BMC Med.* 2020;18:232.
- Van Der Steen N, Lyu Y, Hitzler AK, Becker AC, Seiler J, Diederichs S. The circular rna landscape of non-small cell lung cancer cells. *Cancer (Basel).* 12. 2020;12:1091.
- Ruan H, Xiang Y, Ko J, Li S, Jing Y, Zhu X, et al. Comprehensive characterization of circular rnas in ~1000 human cancer cell lines. *Genome Med.* 2019;11:55.
- Han B, Chao J, Yao H. Circular rna and its mechanisms in disease: from the bench to the clinic. *Pharmacol Ther.* 2018;187:31–44.
- Fang J, Chen W, Meng X. Downregulating circrna\_0044516 inhibits cell proliferation in gastric cancer through mir-149/wnt1/ $\beta$ -catenin pathway. *J Gastrointest Surg.* 2021;25:1696–705.
- Jiang J, Lin H, Shi S, Hong Y, Bai X, Cao X. Hsa\_circrna\_0000518 facilitates breast cancer development via regulation of the mir-326/fgfr1 axis. *Thorac Cancer.* 2020;11:3181–92.
- Liu Z, Yu Y, Huang Z, Kong Y, Hu X, Xiao W, et al. Circrna-5692 inhibits the progression of hepatocellular carcinoma by sponging mir-328-5p to enhance dab2ip expression. *Cell Death Dis.* 2019;10:900.
- Zhou N, Wang W, Xu C, Yu W. Circular rna plec acts as a sponge of microRNA-198 to promote gastric carcinoma cell resistance to paclitaxel and tumorigenesis. *Pathol Res Pract.* 2021;224:153487.
- Gu R, Shao K, Xu Q, Zhao X, Qiu H, Hu H. Circular rna hsa\_circ\_0008003 facilitates tumorigenesis and development of non-small cell lung carcinoma via modulating mir-488/znf281 axis. *J Cell Mol Med.* 2022;26:1754–65.
- Zhao Y, Lu G, Ke X, Lu X, Wang X, Li H, et al. Mir-488 acts as a tumor suppressor gene in gastric cancer. *Tumour Biol.* 2016;37:8691–8.
- Li C, Zhang L, Meng G, Wang Q, Lv X, Zhang J, et al. Circular rnas: Pivotal molecular regulators and novel diagnostic and prognostic biomarkers in non-small cell lung cancer. *J Cancer Res Clin Oncol.* 2019;145:2875–89.
- Michaelidou K, Agelaki S, Mavridis K. Molecular markers related to immunosurveillance as predictive and monitoring tools in non-small cell lung cancer: recent accomplishments and future promises. *Expert Rev Mol Diagn.* 2020;20:335–44.
- Tang X, Ren H, Guo M, Qian J, Yang Y, Gu C. Review on circular rnas and new insights into their roles in cancer. *Comput Struct Biotechnol J.* 2021;19:910–28.
- Wang T, Wang X, Du Q, Wu N, Liu X, Chen Y, et al. The circrna circp4hb promotes nscl aggressiveness and metastasis by sponging mir-133a-5p. *Biochem Biophys Res Commun.* 2019;513:904–11.
- Zhu X, Han J, Lan H, Lin Q, Wang Y, Sun X. A novel circular rna hsa\_circrna\_103809/mir-377-3p/got1 pathway regulates cisplatin-resistance in non-small cell lung cancer (nscl). *BMC Cancer.* 2020;20:1190.
- Oliveto S, Mancino M, Manfrini N, Biffo S. Role of microRNAs in translation regulation and cancer. *World J Biol Chem.* 2017;8:45–56.
- Zhong S, Golpon H, Zardo P, Borlak J. Mirnas in lung cancer. A systematic review identifies predictive and prognostic mirna candidates for precision medicine in lung cancer. *Transl Res.* 2021;230:164–96.
- Liu C, Yang H, Xu Z, Li D, Zhou M, Xiao K, et al. MicroRNA-548I is involved in the migration and invasion of non-small cell lung cancer by targeting the akt1 signaling pathway. *J Cancer Res Clin Oncol.* 2015;141:431–41.
- Jia C, Yao Z, Lin Z, Zhao L, Cai X, Chen S, et al. Circnfatc3 sponges mir-548i acts as a cerna to protect nfatc3 itself and suppressed hepatocellular carcinoma progression. *J Cell Physiol.* 2021;236:1252–69.
- Xu M, Liang H, Li K, Zhu S, Yao Z, Xu R, et al. Value of kpna4 as a diagnostic and prognostic biomarker for hepatocellular carcinoma. *Aging.* 2021;13:5263–83.
- Yang J, Lu C, Wei J, Guo Y, Liu W, Luo L, et al. Inhibition of kpna4 attenuates prostate cancer metastasis. *Oncogene.* 2017;36:2868–78.
- Wang Y, Zhao W, Zhang S. Stat3-induced upregulation of circccdc66 facilitates the progression of non-small cell lung cancer by targeting mir-33a-5p/kpna4 axis. *Biomed Pharmacother.* 2020;126:110019.
- Li X, Yu M, Yang C. Yy1-mediated overexpression of long noncoding rna mcm3ap-as1 accelerates angiogenesis and progression in lung cancer by targeting mir-340-5p/kpna4 axis. *J Cell Biochem.* 2020;121:2258–67.

**How to cite this article:** Yang W, Yao Y, Yang S, Ke Y. Circular RNA hsa\_circ\_0008003 promotes the progression of non-small-cell lung cancer by sponging miR-548I and regulating KPNA4 expression. *Thorac Cancer.* 2023;14(6):544–54. <https://doi.org/10.1111/1759-7714.14777>